http://www.jourmag.org/index.php/jma

Journal of Magnetism and Its Applications

Received February 17th 2021; received in revised March 6th 2021; accepted April 14th 2021

Research articles

Local Structure and Magnetism of $LiFeSi_{0.01}P_{0.99}O_4/C$ as a Cathode Material on Lithium-Ion Battery

Vera Laviara Maghfirohtuzzoimah[1], Sahara Hamas Intifadhah[1], Pelangi Az-zahra[1], Wantana Klysubun[2], Dita Puspita Sari[3,4], Isao Watanabe[4], Mochamad Zainuri[1], Fahmi Astuti[1,4]*

[1]Department of Physics, Faculty of Science and Data Analytics, Institut Teknologi Sepuluh Nopember, Surabaya 60111, Indonesia
[2]Synchotron Light Research Institute, Moo 6 University Ave, Muang, Nakhon Ratchasima 30000, Thailand
[3]Graduate School of Engineering and Science, Shibaura Institute of Technology, Saitama 337-8570, Japan
[4]Meson Science Laboratory, RIKEN Nishina Center, Wako, Saitama 351-0198, Japan

Article info

Keywords:
Cathode material
Lithium-ion battery
Local structure
Oxidation state
X-ray absorption spectroscopy
Magnetism

Abstract

The oxidation state and local structure of $LiFeSi_{0.01}P_{0.99}O_4/C$ composites as a cathode on lithium-ion battery were investigated by Fe K-edge X-ray Absorption Near Edge Spectroscopy (XANES) and Extended X-ray Absorption Fine Structure (EXAFS). The $LiFeSi_{0.01}P_{0.99}O_4/C$ sample was prepared by solid-state reaction process. Based on the XANES analysis, the absorption of edge energy (E_0) of the sample was 7124.92 eV. In addition, linear combination fitting (LCF) analysis of XANES confirmed the oxidation state of iron mixture of 2+ and 3+ as the effect of silicon doped in $LiFePO_4$. The Fourier Transform (FT) of the Fe K-edge EXAFS fitting analysis showed that the nearest neighbors surrounding atom Fe were the main peak with high intensity that confirmed Fe-O bond; the second and third peak with lower intensity confirmed Fe-P and Fe-Fe bonds, respectively. In addition, the SQUID magnetometer result of $LiFeSi_{0.01}P_{0.99}O_4/C$ indicated the antiferromagnetic order temperature of $LiFeSi_{0.01}P_{0.99}O_4/C$ at ~51 K with the indication of the presence of impurity and structural distortion.

1. Introduction

Lithium-ion batteries have stable cycle performance and higher energy density, so promising as power system that have been used in electrical vehicles, portable devices, grid energy storage, etc. [1]. The main component in lithium-ion batteries is cathode material since it is related to the battery capacity, cycle life, and safety. One of cathodes being investigated and commercialized is $LiFePO_4$ that has intrinsic structural and chemical stability so that it is safe and has long cycle life. However, $LiFePO_4$ has poor electronic conductivity (~10^{-9} S cm^{-1}) and low ionic diffusivity (10^{-13} to 10^{-16} cm^2s^{-1}) [2]. Furthermore, to improve the performance of $LiFePO_4$, there are some techniques that can be used, such as reducing particle size, carbon coating, and atomic doping [3].

Reducing particle size is one of the effective ways to increase electronic conductivity. It causes smaller particle size, so lithium ions migrate faster in insertion process because of the reduction of transport distance [4]. Carbon coating is one of the most important techniques used to improve conductivity. The carbon source used as coating such as acetylene black, sucrose, and glucose; however, glucose is better to increase specific surface area in $LiFePO_4$ as a composite [5].

Previously, Amin et al. studied that doping Si to site P in single crystal $LiFePO_4$ was thermodynamically possible. There is no abrupt effect of silicon doping to the crystal structure of $LiFePO_4$ [6]. Furthermore, doping Si to site P in $LiFePO_4$ is able to improve the electronic conductivity. The measurement to verify the sample quality and improvement of the performance of cathode $LiFePO_4$ along with doping are very important such as X-Ray Diffraction (XRD), Scanning Electron Microscopy (SEM), Transmission Electron Microscopy (TEM), Raman spectra, charge-discharge (CD), cyclic voltammetry (CV), and Electrochemical Impedance Spectroscopy (EIS) [7, 8]. In further study, X-ray absorption spectroscopy (XAS) is a powerful technique to probe electronic structure, local structure, and identify the presence of small amount doping on $LiFePO_4$. The information about oxidation state is investigated by X-ray Absorption Near Edge Spectroscopy (XANES) and local structure is investigated by Extended X-ray Absorption Fine Structure (EXAFS) [9]. Furthermore, the use of magnetic characterization in cathode battery materials, especially $LiFePO_4$, is also significant to monitor the sample purity and structural defect of materials [10]. In this study, we investigate the local structure and magnetism of $LiFePO_4$ with doping Si = 1% by X-Ray Absorption Spectroscopy (XAS) and SQUID magnetometer.

2. Experimental Methods

$LiFePO_4$ with doping Si 1% was synthesized via a solid-state reaction. The starting material to obtain $LiFeSi_{0.01}P_{0.99}O_4$ as precursor were Li_2CO_3 (Merck, 99.9%), Fe_2O_3 (technical, 99%), $(NH_4)_2HPO_4$ (Merck, 99.9%), and SiO_2 (Merck 99.9%). The precursor crushed into powders with mortar continued by a ball-milling process with zirconia balls (the precursor ratio: zirconia ball is 1:5) for 10 hours at 150 rpm and dried at 80°C. After that, the sample was annealed at 700°C for 10 hours at nitrogen atmosphere. The sample was coated with 11 wt% glucose $C_6H_{12}O_6$ (technical, 99%) as carbon coating and continued by the carburation process at 450°C for 2 hours under nitrogen atmosphere so that produced $LiFeSi_{0.01}P_{0.99}O_4/C$ (LFP-Si1%). The details of experimental and characterization of XRD, SEM, cyclic voltammetry, and charge/discharge can be referred to the previous work on the reference [8].

In this study, the sample was measured using XAS instruments, including XANES and EXAFS at beamline 8 in Synchrotron Light Research Institute (SLRI) Thailand. Fe K-edge spectra were collected in the range energy 7 keV to 8 keV [11]. The XANES and EXAFS data were analyzed with ATHENA and ARTEMIS programs by IFEFFIT [12]. In addition, to probe magnetic properties of LFP-Si1%, the SQUID measurement was performed with the temperature range of 2-300 K under a magnetic field of 10 kOe [13].

*Corresponding author
Email: fahmia@physics.its.ac.id

DOI: 10.53533/JMA.v1i1.6

3. Results and Discussion

The information of oxidation state from XANES data has been processed using ATHENA program. Fig.1(a). displays the normalization absorption Fe K-edge XANES spectra of LFP-Si1% with data standard including Fe foil (0), FeO (+2), Fe_2O_3 (+3), and $FePO_4$ (+3) as compared with the LFP-Si1%. The regions of XANES data are pre-edge (symbolized (*)) that explain the transition electron from the orbital 1s to the 3d from the Fe absorber and the edge (symbolized (#)), which corresponds to the first derivative normalized, indicating the minimum energy needed to remove the photoelectron from the absorbing showed in Fig.1(b). The pre-edge and edge region can be used to determine the oxidation state of the sample. The increasing of oxidation state is related to the higher absorption edge value. The energy absorption edge (E_0) of LFP-Si1% is 7124.92 eV in between FeO (E_0 = 7120.02 eV) and Fe_2O_3 (E_0 = 7125.68 eV) that have oxidation state 2+ and 3+, respectively. The prediction of oxidation state can be estimated by interpolation technique using E_0 value of LFP-Si1% in comparison with that of standard data Fe foil, FeO, Fe_2O_3, and $FePO_4$; which result in oxidation state of LFP-Si1% about +2.64.

In addition, to confirm the oxidation state composition of LFP-Si1%, linear combination fitting (LCF) in ATHENA was used. The standard data used in LCF are FeO and Fe_2O_3 since the fitting using these two compounds obtained the best fitting result. The LCF result of the composition of oxidation state Fe_2O_3 (3+) is 73.3% and FeO (2+) is 26.7%. The analysis using interpolation exhibits good agreement with LCF result since the oxidation state of multivalence Fe is in between 2+ and 3+ [14–16]. The multivalence of Fe, which triggered the existence of a small magnetic polaron, is responsible for the interplay between electronic conductivity and magnetism in $LiFePO_4$ [17].

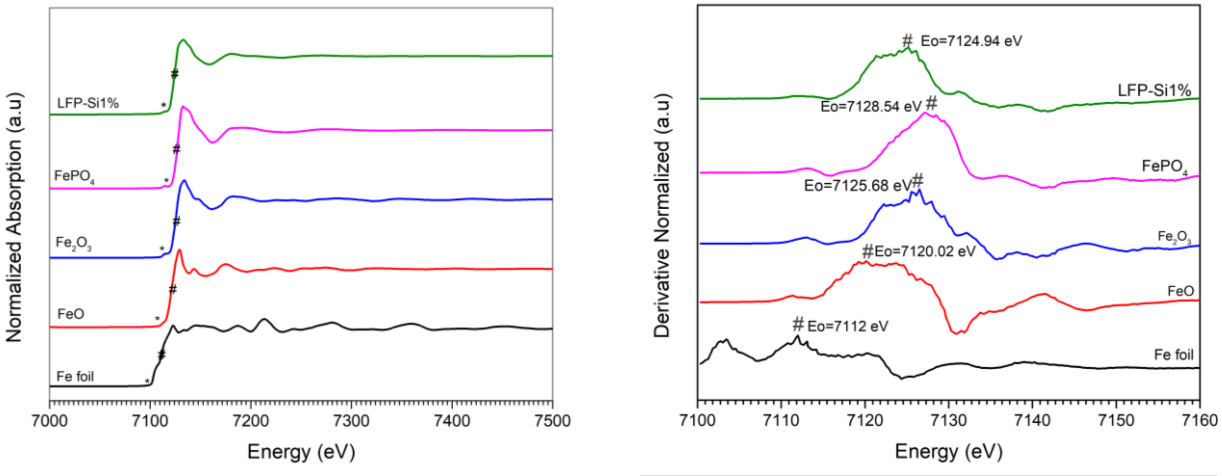

(a) (b)

Fig. 1. (a) Normalized absorption Fe K-edge spectra of $LiFeSi_{0.01}P_{0.99}O_4/C$, (b) Derivative normalized absorption Fe K-edge spectra of $LiFeSi_{0.01}P_{0.99}O_4/C$

The analysis to study local structure of LFP-Si1% can determine the nearest neighbor and interatomic distance using Fe K-edge of XAS. The fitting of EXAFS data analysis prefers structure $LiFePO_4$ model taken from crystallography.net with Crystallography Open Database (COD) ID 1101111. The model of $LiFePO_4$ (olivine) doping Si (LFP-Si1%) in EXAFS fitting obtained from the replacement of scattering paths P_1 with Si in ARTEMIS program. Fig.2 shows the EXAFS data fitting of LFP-Si1%. In Fig. 2, the upper curve is the magnitude of Fourier Transform (FT) EXAFS data and the lower curve is either real or imaginary part of the FT data to determine radial distance in R-space [15, 18].

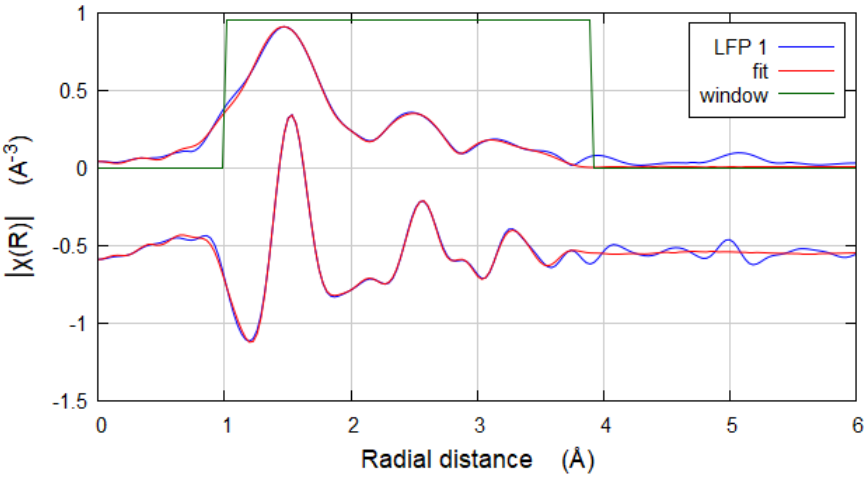

Fig. 2. Fitting EXAFS data $LiFeSi_{0.01}P_{0.99}O_4/C$ in Fe K-edge

Based on the analysis of Fourier transform (FT) of EXAFS spectra of the sample presented in $k^3\chi(k)$ in Fig.3, the nearest neighbors in surrounding atom Fe consist of: the main peak with high intensity confirms as Fe-O bond and the second and third peak with lower intensity confirm as Fe-P and Fe-Fe bonds, respectively. The local structure of LFP-Si1% results with output parameters (CN, σ^2, and R-factor) to obtain the distance between Fe and nearest neighbor are presented in Table 1. The local structure of LFP-Si1% confirms Fe binding six atom O in octahedral sites (FeO_6) and minor changes in the interatomic distance through distortion were found compared to that $LiFePO_4$ without doping based on the previous studies [9, 19]. The distortion atom of $LiFePO_4$ by Si doping could affect its structural stability, which further influences its electrochemical performance. This can be a reason for the enhancement of electrochemical performance of $LiFePO_4$ with silicon doping, as reported by Zainuri et al. [8].

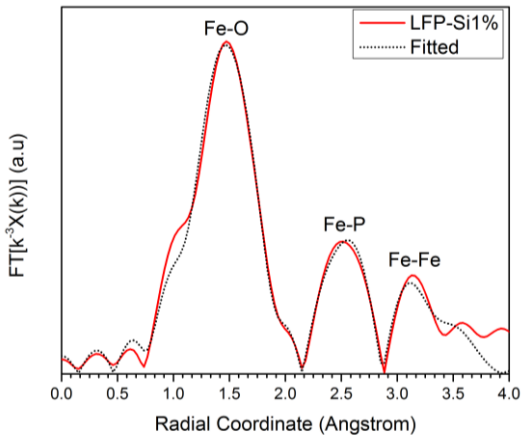

Fig. 3. *R*-Space EXAFS data and the fitted data of $LiFeSi_{0.01}P_{0.99}O_4/C$ in Fe K-edge

Table 1. Structural parameters of $LiFeSi_{0.01}P_{0.99}O_4/C$ from EXAFS data fitting

Z_a-Z_b	CN	R (Å)	σ^2(Å^2)	R-factor
Fe-O_1	2	2.035	0.004	0.006
Fe-O_2	1	1.898	0.004	
Fe-O_3	1	2.192	0.005	
Fe-O_4	2	2.517	0.042	
Fe-Si	1	2.886	0.014	
Fe-P_2	1	3.444	0.008	
Fe-P_3	3	3.221	0.013	
Fe-Fe	4	3.769	0.022	

*Za-Zb represent central absorber and scattering atom correlation, CN (coordinate number), R (interatomic distance), σ^2 (Debye-Waller factor)

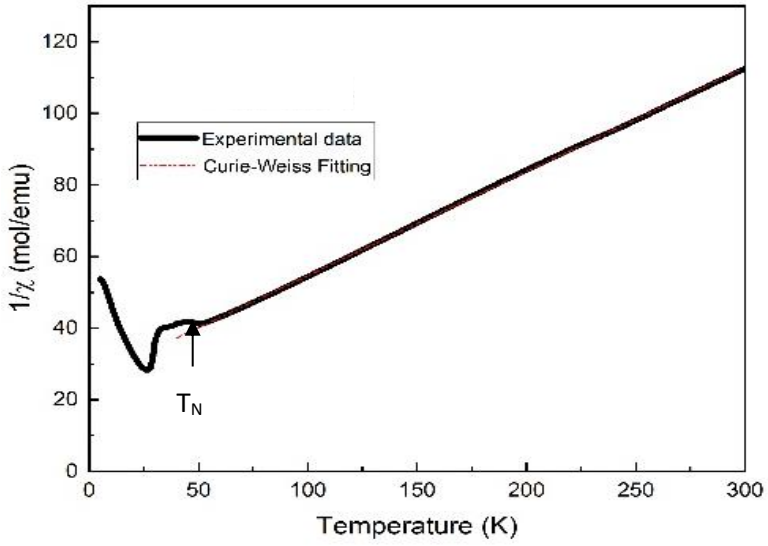

Fig. 4. SQUID magnetometer result of $LiFeSi_{0.01}P_{0.99}O_4/C$

Figure 4 displays the temperature dependence of inverse magnetic susceptibility, χ^{-1}, of $LiFeSi_{0.01}P_{0.99}O_4/C$ under an applied magnetic field of 10 kOe. There are two anomalies observed from the temperature dependence of χ^{-1}. One is ~51 K which indicates the antiferromagnetic ordering temperature (T_N) of olivine $LiFePO_4$ as also reported by Julien et al. [20], while the other is ~28 K which could correspond to nasicon $Li_3Fe_2(PO_4)_3$ [21]. The existence of $Li_3Fe_2(PO_4)_3$ as a secondary phase was also confirmed from the XRD results in Ref [8]. It has been reported that nasicon $Li_3Fe_2(PO_4)_3$ is the most common impurity in $LiFePO_4$ [10]. Accordingly, the temperature dependence of the magnetic susceptibility was analyzed by using the Curie-Weiss law. The Curie-constant (C), effective magnetic moments (μ_{eff}) and Curie-Weiss temperature (Θ) were estimated to be 3.44 emu.K/mol, 5.23 μ_B and - 88.14 K, respectively. The large value of magnetic moments is attributed to the presence of Fe ions. In olivine $LiFePO_4$, the purest sample has μ_{eff} = 4.98 μ_B, while the value of μ_{eff} in such impure $LiFePO_4$ is estimated to be in the range of 4.9-5.5μ_B [10]. It is related to the total spin in $LiFePO_4$ with S=2; hence the spin-only value is ~4.9 μ_B while the presence of orbital contributions (S = 2; L = 2) results in μ_{eff} = 5.48 μ_B. The high-spin in $LiFePO_4$ is able to trigger the incomplete quenching of orbital moment and further result in the orbital contributions which is sensitive to the distortion of octahedral symmetry of FeO_6. The silicon doping on $LiFePO_4$ possibly affects further the distortion in relation to its atomic distance as shown in XAS result which could influence its electrochemical performance. The characterization techniques to study magnetic properties on batteries, especially to highlight their sensitivity to the presence of impurity and structural defect, even beyond the XRD technique, is the goal for the next study.

4. Conclusions

The analysis of $LiFeSi_{0.01}P_{0.99}O_4/C$ composites as lithium-ion battery cathode studied by XAS has been done in this study. The multivalence of Fe with oxidation state 2+ and 3+ was obtained in LFP-Si1% confirmed by linear combination fitting (LCF) and interpolation technique. Furthermore, silicon doping in $LiFePO_4$ could generate the changes in interatomic distance of the sample which further affect the electrochemical performance. The nearest neighbor from Fe K-edge as central absorber was found as Fe-O bond with higher intensity and Fe-

P and Fe-Fe as second and third bonds with lower intensity. The Neel temperature (T_N) of $LiFeSi_{0.01}P_{0.99}O_4$/C was estimated to be ~51 K based on SQUID magnetometer result, with the indication of the presence of impurity and structural distortion due to the orbital contributions.

Acknowledgements

This work was supported by Dana Lokal ITS Penelitian Doktor Baru No: 855/PKS/ITS/2020, Lembaga Ilmu Pengetahuan Indonesia (LIPI). The authors thank the staff at beamline 8, Synchrotron Light Resource Institute (SLRI), for supporting XAS data collection.

References

[1] K. Liu, Y. Liu, D. Lin, A. Pei, and Y. Cui, "Materials for lithium-ion battery safety," *Sci. Adv.*, vol. 4, no. 6, p. eaas9820, 2018.
[2] J. Wang and X. Sun, "Understanding and recent development of carbon coating on $LiFePO_4$ cathode materials for lithium-ion batteries," *Energy Environ. Sci.*, vol. 5, no. 1, pp. 5163–5185, 2012.
[3] W.-J. Zhang, "Structure and performance of $LiFePO_4$ cathode materials: A review," *J. Power Sources*, vol. 196, no. 6, pp. 2962–2970, 2011.
[4] G. T.-K. Fey, Y. G. Chen, and H.-M. Kao, "Electrochemical properties of $LiFePO_4$ prepared via ball-milling," *J. Power Sources*, vol. 189, no. 1, pp. 169–178, 2009.
[5] Z. Chen, H. Zhu, S. Ji, R. Fakir, and V. Linkov, "Influence of carbon sources on electrochemical performances of $LiFePO_4$/C composites," *Solid State Ionics*, vol. 179, no. 27–32, pp. 1810–1815, 2008.
[6] R. Amin *et al.*, "Silicon-Doped LiFePO4 Single Crystals: Growth, Conductivity Behavior, and Diffusivity," *Adv. Funct. Mater.*, vol. 19, no. 11, pp. 1697–1704, 2009.
[7] J.-W. Zhao, S.-X. Zhao, X. Wu, H.-M. Cheng, and C.-W. Nan, "Double role of silicon in improving the rate performance of $LiFePO_4$ cathode materials," *J. Alloys Compd.*, vol. 699, pp. 849–855, 2017.
[8] M. Zainuri and P. A. Zahra, "Active Materials $LiFeSi_xP_{1-x}O_4$/C as Lithium Ion Battery Cathode with Doping Variations Si Ions ($0 \leq x \leq 0, 06$)," in *Key Engineering Materials*, 2020, vol. 860, pp. 75–80.
[9] M. Norouzi Banis *et al.*, "Chemical speciation and mapping of the Si in Si doped LFP ingot with synchrotron radiation technique," *Can. J. Chem. Eng.*, vol. 97, no. 8, pp. 2211–2217, 2019.
[10] N. A. Chernova, G. M. Nolis, F. O. Omenya, H. Zhou, Z. Li, and M. S. Whittingham, "What can we learn about battery materials from their magnetic properties?," *J. Mater. Chem.*, vol. 21, no. 27, pp. 9865–9875, 2011.
[11] W. Klysubun *et al.*, "Upgrade of SLRI BL8 beamline for XAFS spectroscopy in a photon energy range of 1–13 keV," *Radiat. Phys. Chem.*, vol. 175, p. 108145, 2020.
[12] B. Ravel and M. Newville, "ATHENA, ARTEMIS, HEPHAESTUS: data analysis for X-ray absorption spectroscopy using IFEFFIT," *J. Synchrotron Radiat.*, vol. 12, no. 4, pp. 537–541, 2005.
[13] K. Zaghib *et al.*, "Optimized electrochemical performance of $LiFePO_4$ at 60 °C with purity controlled by SQUID magnetometry," *J. Power Sources*, vol. 163, no. 1, pp. 560–566, 2006.
[14] H. Husain *et al.*, "The structural and magnetic characterization of ironstone-derived magnetite ceramic nanopowders," *J. Mater. Sci. Mater. Electron.*, vol. 31, no. 15, pp. 12398–12408, 2020.
[15] D. C. Koningsberger and R. Prins, "X-ray absorption: principles, applications, techniques of EXAFS, SEXAFS, and XANES," 1988.
[16] S. D. Kelly, D. Hesterberg, and B. Ravel, "Analysis of soils and minerals using X-ray absorption spectroscopy," *Methods soil Anal. part 5—mineralogical methods*, vol. 5, pp. 387–463, 2008.
[17] K. Zaghib, A. Mauger, J. B. Goodenough, F. Gendron, and C. M. Julien, "Electronic, optical, and magnetic properties of $LiFePO_4$: small magnetic polaron effects," *Chem. Mater.*, vol. 19, no. 15, pp. 3740–3747, 2007.
[18] K.-F. Hsu *et al.*, "Formation mechanism of $LiFePO_4$/C composite powders investigated by X-ray absorption spectroscopy," *J. Power Sources*, vol. 192, no. 2, pp. 660–667, 2009.
[19] C. M. Julien, K. Zaghib, A. Mauger, and H. Groult, "Enhanced electrochemical properties of $LiFePO_4$ as positive electrode of Li-ion batteries for HEV application," 2012.
[20] A. Ait-Salah, P. Jozwiak, J. Garbarczyk, F. Gendron, A. Mauger, and C. M. Julien, "Magnetic properties of orthorhombic $Li_3Fe_2(PO_4)_3$ phase," in *Electrochem Soc Symp Proc*, 2006, vol. 19, pp. 173–181.
[21] F. Astuti *et al.*, "Anionogenic magnetism combined with lattice symmetry in alkali-metal superoxide RbO_2," *J. Phys. Soc. Japan*, vol. 88, no. 4, p. 43701, 2019.